AIAA JOURNAL
Vol. 48, No. 1, January 2010

Excess Broadband Noise Observed with Overexpanded Jets

K. B. M. Q. Zaman,* James E. Bridges,† and C. A. Brown‡
NASA John H. Glenn Research Center at Lewis Field, Cleveland, Ohio 44135

DOI: 10.2514/1.43383

Results of an experiment on the characteristics of an excess noise occurring with convergent–divergent nozzles in the overexpanded regime are presented in this paper. Data are obtained with five convergent–divergent nozzles and a convergent nozzle, all having the same exit diameter. The results clearly establish that, relative to the convergent case and at same pressure ratios, the convergent–divergent nozzles are noisier in the low Mach number range of the overexpanded regime. This is evidenced from the directivity patterns as well as the overall radiated sound power. The excess noise is broadband in nature and is found to be more pronounced with nozzles having a higher design Mach number or larger half angle of the divergent section. It appears to occur when a shock resides within the divergent section and results from random unsteady motion of the shock.

I. Introduction

A BROADBAND noise component occurring in the over-expanded flow regime with convergent–divergent (C–D) nozzles was investigated earlier in [1]. Relative to a convergent nozzle, at the same pressure ratios, this excess broadband noise (to be referred to in the following as EBBN) can lead to a large increase in the overall sound pressure levels (OASPLs). Several features distinguish it from the more familiar broadband shock associated noise (BBSN). The phenomenon, as understood thus far, is best explained with the help of the schematic in Fig. 1. Following [2], data trends for OASPL are shown as a function of M_j for various cases; here, M_j is the fully expanded jet Mach number defined in the next section. The dotted line represents turbulent mixing noise. This curve would be obtained if, at each M_j, an appropriate C–D nozzle were used to obtain perfectly expanded flow. Results from a convergent nozzle are represented by the dashed curve, and those from a given C–D nozzle are shown by the solid curve. At the design Mach number (fully expanded condition), the C–D nozzle generates noise due only to turbulent mixing. Relative to this point, on either the left (overexpanded condition) or the right (underexpanded condition), the C–D nozzle exhibits higher levels due to BBSN. In the schematics used by Tam and Tanna [2] and Tam [3], the levels for the convergent nozzle were shown to be approximately the same as those for the C–D nozzle on the low end of the M_j range. The focus in those earlier studies was on BBSN occurring at higher M_j, and attention was not paid to the range of M_j below about 1.2. It is in this range the intensities are found to be much larger than the convergent case. The excess level is sketched by the solid line and indicated by an arrow.

As identified in [1], various features of EBBN distinguished it from BBSN. Unlike the latter, it was observed to persist at shallow polar locations. There was no noticeable shift of the spectral content in frequency between a shallow polar location and locations normal to the jet axis. The amplitudes of EBBN were found to be more pronounced with nozzles having a larger half angle of the divergent section. The source of EBBN appeared to be tied to unsteady shock motion within the divergent section.

Although a lot was learned in [1], the full characteristics of EBBN remained uncharted, and its mechanism not clearly understood. The following aspects of the experiment reported in [1] left some ambiguities:

1) The study was conducted with tiny nozzles having nominal diameters of 0.3 in..

2) The nozzles had simple conical divergent sections. Therefore, the flow was never perfectly expanded at the design Mach number, and the dip in the OASPL curve (Fig. 1) was never observed. It was not clear if EBBN would occur with well-designed C–D nozzles.

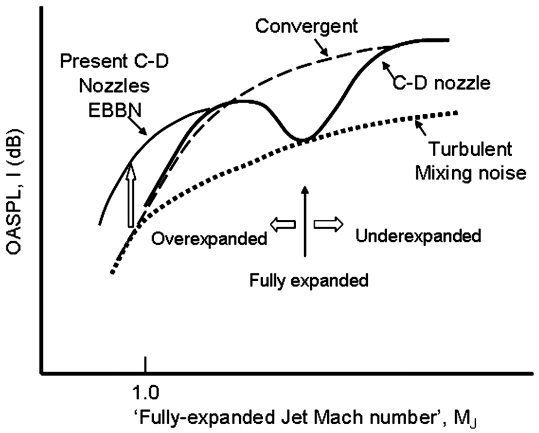

Fig. 1 Schematic of OASPL vs M_j for C–D and convergent nozzles (after [2]).

Fig. 2 The SHJAR viewed from above. The 24 microphone array is located on a 100 in. radius, covering angles 15 deg $<\theta<$ 130 deg; θ is referenced to the downstream jet axis. The nozzle and microphones are eight feet above the wedge tips.

Presented as Paper 0289 at the 47th AIAA Aerospace Sciences Meeting, Orlando, FL, 5–8 January 2009; received 26 January 2009; accepted for publication 19 September 2009.

*Aerospace Engineer, Inlet and Nozzle Branch, Aeropropulsion Division. Associate Fellow AIAA.

†Aerospace Engineer, Acoustics Branch, Aeropropulsion Division. Associate Fellow AIAA.

‡Aerospace Engineer, Acoustics Branch, Aeropropulsion Division.

Table 1 Nozzle dimensions (in inches) and other characteristics; all nozzles are 7.5 in. long and have an exit diameter of $D_e = 2$ in.. M_j sub and M_j shock are values of M_j when the shock is at the throat and at the exit per 1-D analysis, and M_D is the design Mach number. Corresponding NPR values are shown in the last three columns

Nozzle	Throat diameter, D_t	Divergent section length	M_D	M_j sub	M_j shock	NPR design	NPR sub	NPR shock
M10	2	0	1.0	——	——	1.893	——	——
M14	1.8952	1.832	1.4	0.674	0.784	3.182	1.355	1.501
M16	1.7900	2.382	1.6	0.553	0.789	4.251	1.231	1.508
M18	1.6702	2.630	1.8	0.454	0.842	5.746	1.152	1.590
M22	1.4148	3.351	2.2	0.305	1.026	10.692	1.067	1.952
M28	1.073	4.002	2.8	0.168	1.363	27.138	1.020	3.022

3) The exit diameters of the C–D nozzles varied, and the results were compared with data from a larger convergent nozzle by scaling all data with respect to the throat diameters. It was desirable to compare the intensity levels for nozzles of same size. There also remained some question whether the noise should be scaled with respect to the throat or the exit diameters.

The ambiguities listed in the foregoing provided the motivation to carry out a further study. A set of larger C–D nozzles (all with exit diameters of 2 in.) were fabricated for this purpose. Preliminary acoustic surveys were conducted in a smaller semi-anechoic facility. Subsequently, detailed data were acquired in a larger anechoic facility described in the following. The objective of this paper is to document the results from the latter experiment and provide a discussion with the primary focus on the EBBN.

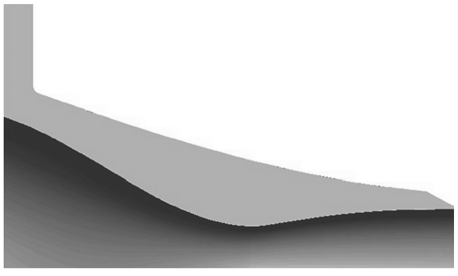

a)

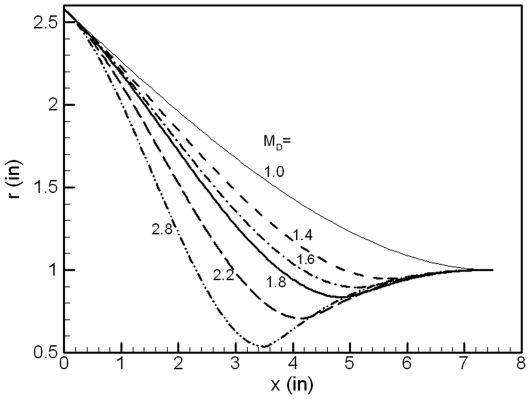

b)

c)

Fig. 3 Nozzles: a) CAD drawing of one of the C–D nozzles, b) internal contours of all nozzles, and c) picture of M22T.

II. Experimental Facility

The data were acquired in the small hot jet acoustic rig (SHJAR) located in the Aeroacoustic Propulsion Laboratory (AAPL) at the NASA John H. Glenn Research Center at Lewis Field (Fig. 2). It is a single flow jet rig that uses 150 psi air supplied by several remotely located compressors. The maximum mass flow rate is 6 lbm/s. The air passes through a baffled muffler and a settling chamber before reaching the nozzle. Two valves (a large main valve and a small vernier valve) regulate the airflow, providing fine control over the entire range of operating conditions. The AAPL, which houses the SHJAR, is a geodesic dome (60 ft radius) lined with sound-absorbing wedges that reduce sound reflection at all frequencies above 200 Hz [4]. The jet exhaust is directed outside through a large door.

Acoustic data in the SHJAR are acquired by an array of 24 microphones. Each microphone is 100 in. away from the nozzle exit. They are spaced at approximately 5 deg intervals from 15 to 130 deg. The angular location θ is referenced to the downstream jet axis. To minimize reflection, six stands (each holding four microphones) are used. Another computer, dedicated to the facilities, records other variables, such as rig temperatures, pressures, and mass flow rate (as well as ambient temperature, pressure, and humidity). A DataMAX® instrumentation recorder (from R.C. Electronics) simultaneously

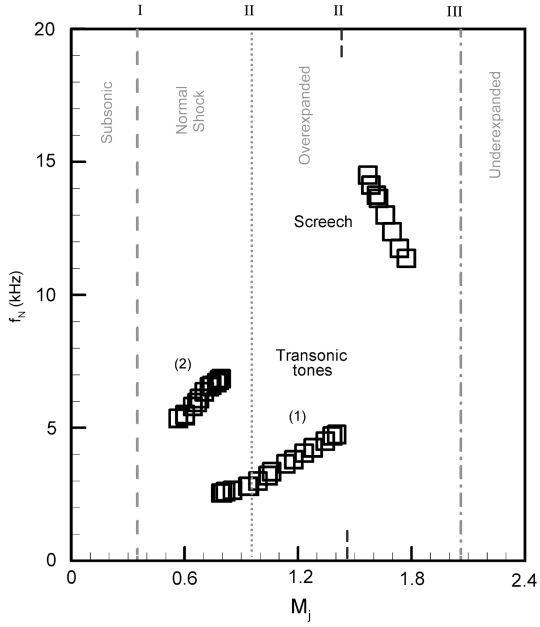

Fig. 4 Variation of frequencies of transonic tone and screech with M_j for a small C–D nozzle ($D_t = 0.3$ in. and $D_e = 0.4$ in.) (from [5]).

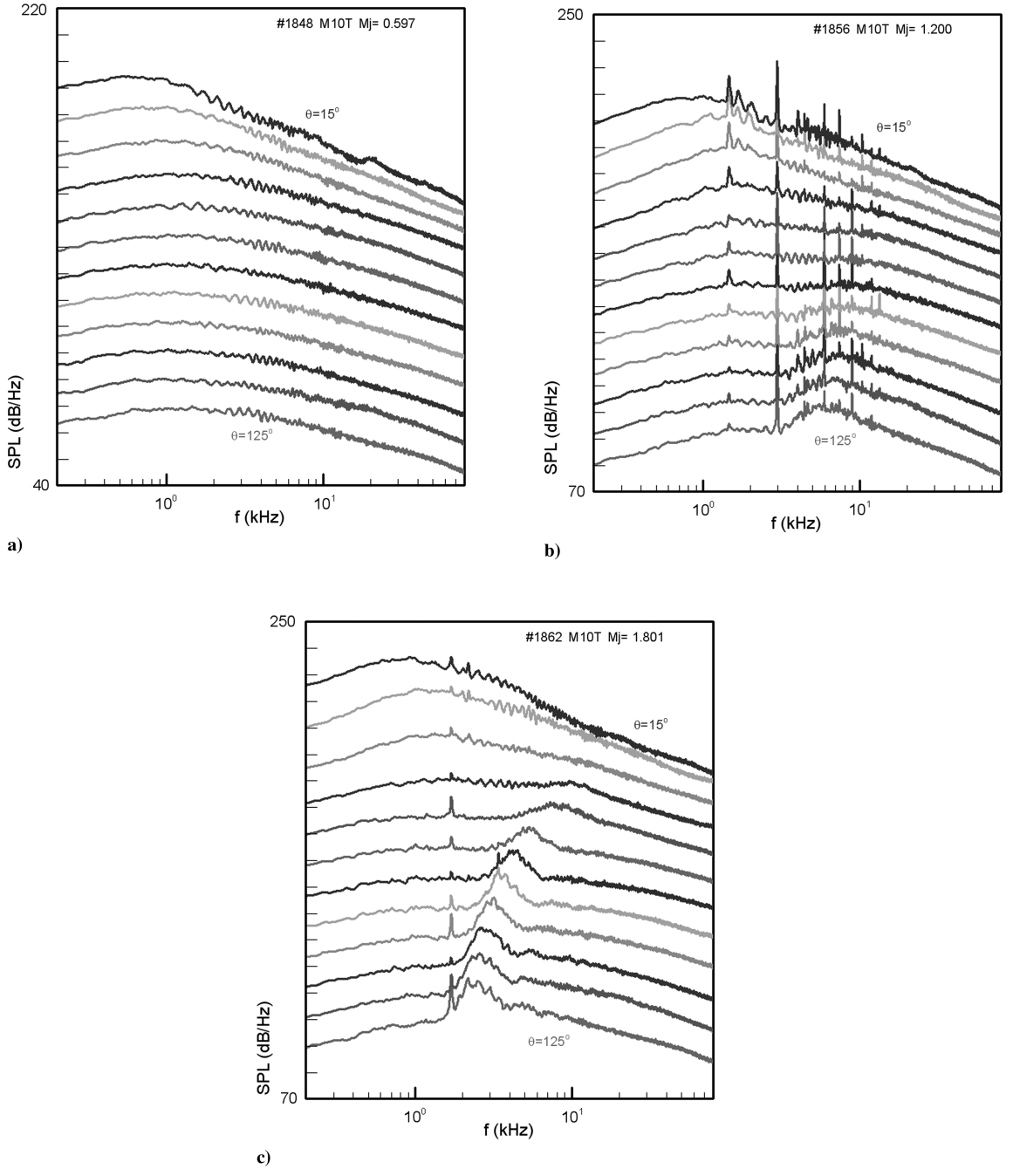

Fig. 5 SPL spectra for nozzle M10T. In each set, data are for different θ at increments of 10 deg. The ordinate pertains to the curve for $\theta = 125$ deg (successive curves shifted by 10 dB).

records data from all microphones, using a 90 kHz low-pass filter and at a sampling rate of 200 kHz. Bruel and Kjaer Nexus™ amplifiers provide the signal conditioning. Eight seconds of data are recorded at each point. Further details of the facility and a description of the tests validating the data system can be found in [4].

Six nozzles are used in the experiment, all having an exit diameter of 2 in. and a length of 7.5 in. The divergent sections are designed following the method of characteristics. The length of the divergent section varies depending on the design Mach number. Thus, the lengths of the convergent section also vary. A fourth-order polynomial fit is used to design the convergent section, matching the slope of the upstream hardware and bringing the slope to zero at the throat. The important dimensions of the six nozzles are given in Table 1.[§]

[§]A suffix T following a nozzle designation will represent a tripped boundary layer.

A computer-aided-design (CAD) drawing of one of the nozzles is shown in Fig. 3a. Figure 3b shows the internal wall contours for all nozzles. A boundary layer trip is applied in order to suppress transonic tones, discussed further in the following. The trip consists of four strips of aluminum tape. Each is 0.625 in. wide at the base and about 0.75 in. long, with the upstream end cut into a triangular shape. The tapes are 0.004 in. thick and applied close to, but sufficiently upstream of, the throat to not affect its diameter. Figure 3c shows a view of the M22T nozzle from the upstream end where the trips are visible. In the following, the fully expanded jet Mach number

$$M_j = \left\{ \left[(p_0/p_a)^{(\gamma-1)/\gamma} - 1 \right] \frac{2}{\gamma - 1} \right\}^{1/2}$$

is used as the independent variable. Here, p_0 and p_a are plenum pressure and ambient pressure, respectively. Note that for imperfectly expanded flows, M_j is a fictitious Mach number. It is

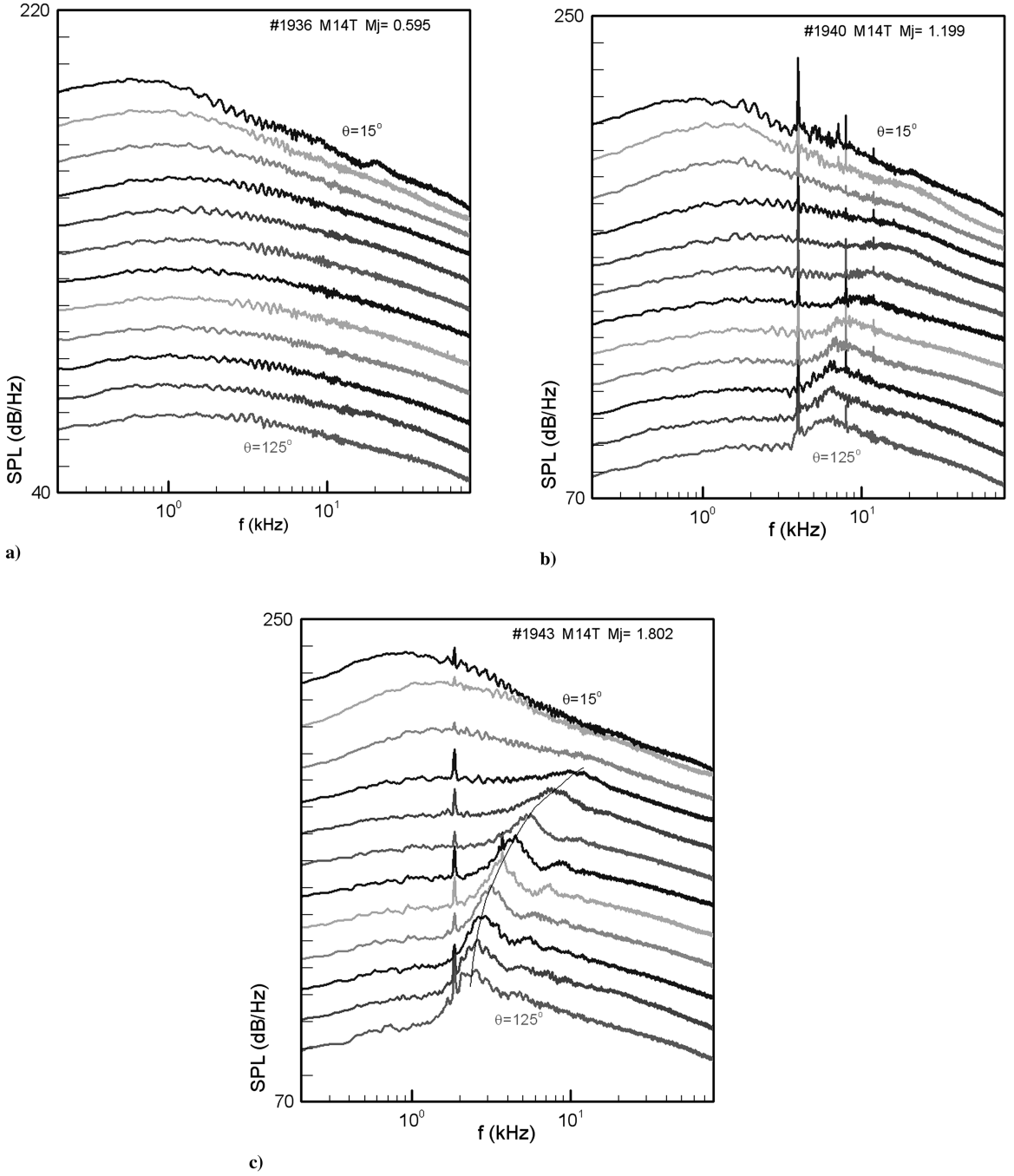

Fig. 6 SPL spectra for nozzle M14T (shown similarly in Fig. 5).

simply a function of nozzle pressure ratio and represents the Mach number at the exit of a nozzle, had the flow expanded fully. In Table 1, the values of M_j for various flow conditions based on one-dimensional (1-D) analysis are shown. The notations are defined in the caption, and the corresponding nozzle pressure ratios (NPR= p_0/p_a) are also shown in the table.

For all of the tripped cases, the spectra of the 24 microphone signals are recorded for 12 values of M_j, covering the range 0.3–2.0. In addition, data are also recorded for the (untripped) M18 and M22 cases. The highest M_j (=2) could not be covered for the convergent and the M14 nozzles because the required mass flow rate exceeded the supply. All noise data are corrected for atmospheric attenuation and referenced to a 1 ft distance from the nozzle. All data pertain to cold flow (i.e., having the total temperature the same everywhere as in the ambient).

It should be mentioned here that, although most data presented in this paper were obtained in the SHJAR, preliminary data were obtained with the same nozzles in a smaller semi-anechoic facility. A set of the preliminary data will be shown to illustrate the facility independence of the phenomenon under investigation. Note also that the earlier results of [1] (first documenting the phenomenon) were obtained in another, even smaller, facility. An interested reader may find descriptions of the latter two facilities in [1,5].

III. Results

To obtain a clear sense of the operating regimes as well as the nature of the transonic tones, first let us consider Fig. 4, reproduced from [5]. The frequencies of sharp tones, observed with a small C–D nozzle while the driving pressure (and thus, M_j) is varied, are plotted. The band of data on the right represents screech, and there are two stages of transonic tones on the left, as indicated. The vertical lines in this figure demarcate flow regimes determined by 1-D nozzle flow analysis, based on the throat-to-exit area ratio. From the left, the first

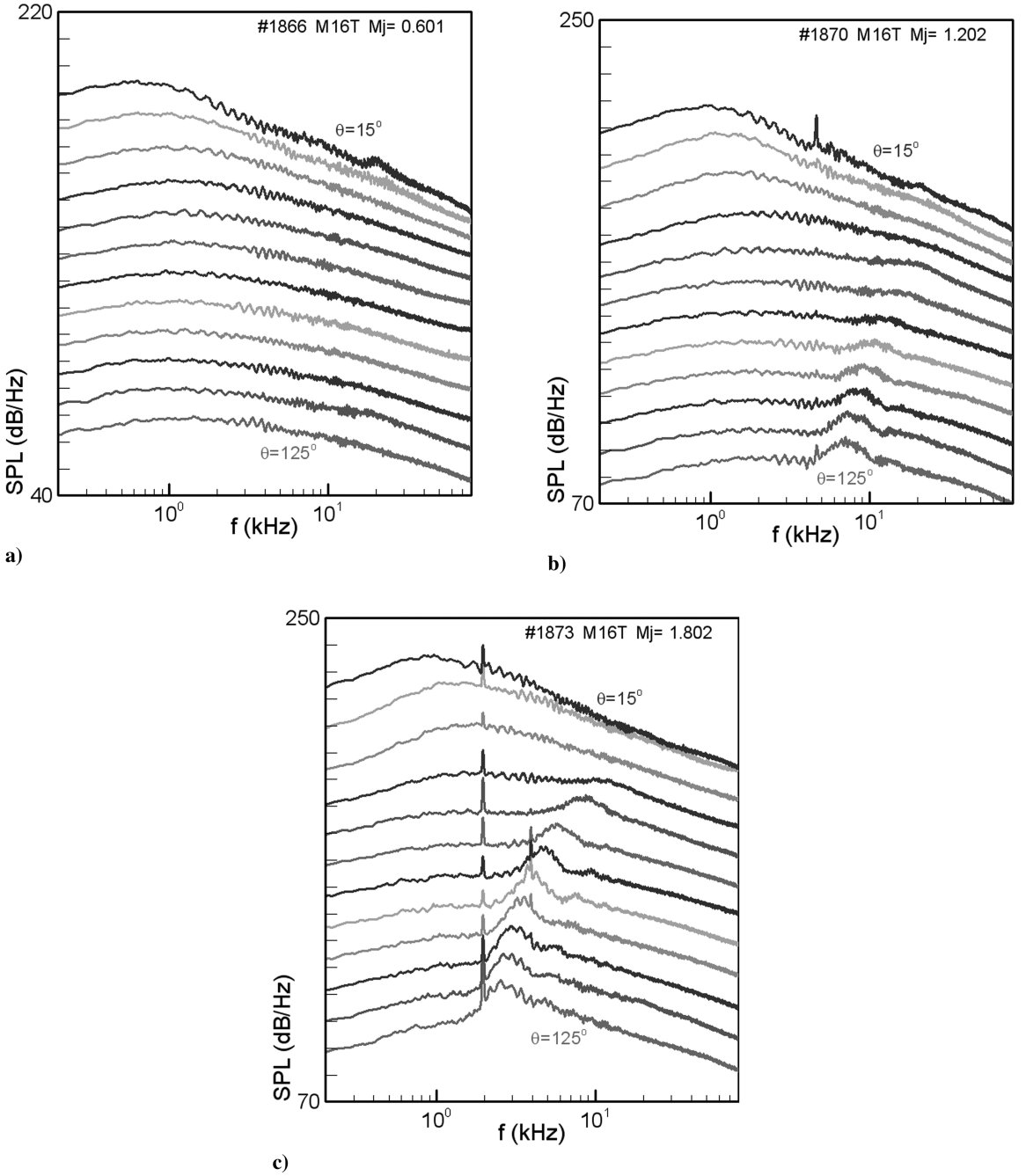

Fig. 7 SPL spectra for nozzle M16T (shown similarly in Fig. 5).

line (I) represents the condition when the throat is just choked, the second line (II) represents when the normal shock is just at the exit, and the third line (III) represents when the flow is perfectly expanded. Thus, to the left of line I, the flow is subsonic; between lines I and II, a shock is expected in the divergent section; between lines II and III, the flow is overexpanded; and to the right of line III, the flow is underexpanded. Whereas boundaries I and III are well represented, it is well known that boundary II is grossly underpredicted by 1-D analysis. In reality, for the nozzle under consideration, boundary II is actually located far to the right at location II'. Thus, the transonic tone can be seen to occur in the regime bounded by I and II' when a shock resides within the divergent section of the nozzle. The section of the nozzle downstream of the shock acts as a resonator, having one end closed and the other open. Fundamental quarter-wave resonance corresponds to stage 1, marked in Fig. 4. Resonance can also occur at odd harmonics, stage 2 in Fig. 4 being the third harmonic (reader may look up [5] for further details).

From the evidence gathered to date [1], it appears that the broadband noise EBBN also takes place in the same flow regime (I–II') when a shock resides within the divergent section. It should be noted that, in order to study the broadband noise, it is desirable that the tones are not present. The transonic tones have been shown to be characteristic of nozzles with smooth interiors. Suitable boundary layer tripping often suppresses the tones. As indicated in Sec. II, most of the data in the following are presented for nozzles with a tripped boundary layer. Here, it is also relevant to note that the flow coming out of the nozzle in the regime bounded by I and II', in the sense of 1-D analysis, may be expected to be subsonic, and true overexpanded flow may be expected only in the range II'–III. In reality, however, when a shock resides within the nozzle, the flow downstream separates, and the ensuing jet contains shocks with characteristics similar to that of an overexpanded jet [1,6]; hence, the justification of the term overexpanded for the flows under consideration.

Representative sound pressure level (SPL) spectra are documented in Figs. 5–11. These are shown as waterfall plots for three values of M_j (=0.6, 1.2, and 1.8). The nozzle configuration and M_j are indicated in the legend of each figure (the first number is a record number retained for tracking purposes and should be ignored by the

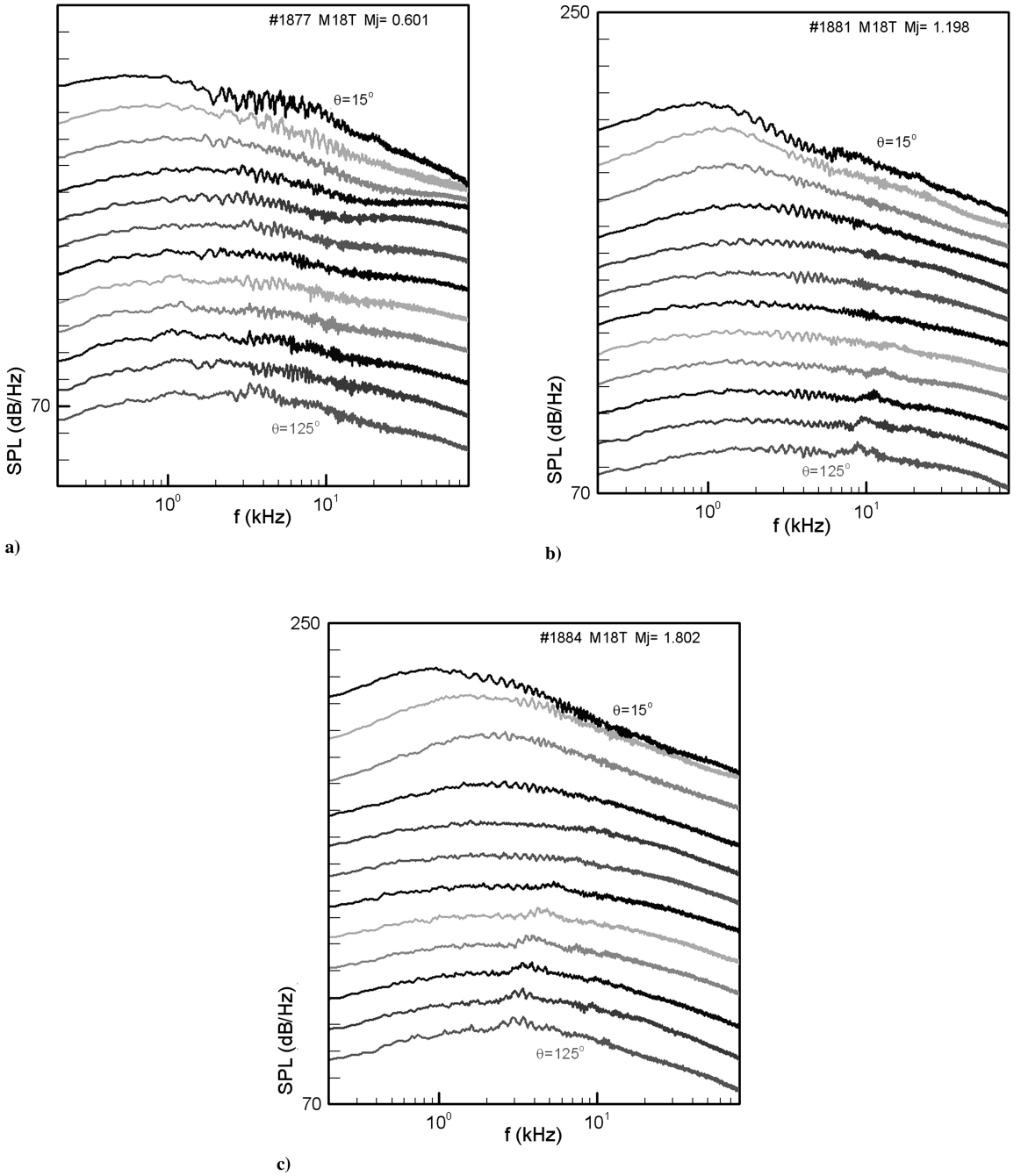

Fig. 8 SPL spectra for nozzle M18T (shown similarly in Fig. 5).

reader). For clarity, only 12 spectral traces from alternate microphones are shown in each figure. The measurement angular location θ is indicated for two traces at the top and bottom; the others are at an interval of 10 deg. Note again that a smaller θ represents a location closer to the downstream end of the jet. In Fig. 5, for the M10T case, the traces are uneventful at the lowest M_j. Screech is noticed at $M_j = 1.2$, whereas screech as well as clear BBSN are visible at the highest M_j. As is well known, the frequency of the BBSN peak increases with decreasing angular location θ. Small amplitude BBSN can also be discerned at $M_j = 1.2$.

Similar trends are seen in Figs. 6 and 7 for the M14T and M16T nozzles, respectively. In Fig. 6, the peaks of BBSN are connected by a smooth curve, as an example; the intersection of such a curve with the individual traces allowed a clearer determination of the frequencies, to be documented in the Appendix. In Fig. 8, for the M18T case, BBSN or screech are practically absent at $M_j = 1.8$ (as expected) because the flow is fully expanded. At $M_j = 0.6$, in Fig. 8, it can be seen that the levels are generally elevated, especially on the high frequency end; compare, for example, the curves for $\theta = 125$ deg between Figs. 7 and 8. At $M_j = 0.6$, the levels rise further with the M22T case in Fig. 9. The elevation of the broadband levels at $M_j = 0.6$ as well as at 1.2, perhaps not completely clear from these plots, is illustrated further in the following. In Fig. 10, for the largest design Mach number case (M28T), the levels have actually fallen back somewhat, and this will also become clear with the following figures.

The transonic tone is clearly seen at the lowest M_j for the untripped M22 nozzle (Fig. 11). The effect of the tripping can be appreciated by comparing it with the corresponding ($M_j = 0.6$) data in Fig. 9. The fundamental tone frequency is 1170 Hz. From the correlations provided in [5], it can be inferred that this is a tone in stage 2. With a half angle of 5 deg for the given nozzle and $M_j = 0.6$, the tone frequency for stage 2 can be calculated as 1120 Hz, agreeing reasonably with the observation. Note that, for $M_j = 0.6$ in Fig. 9, even with the trip, a small peak is observed around 1170 Hz. Similarly, a small peak near the expected transonic tone is also

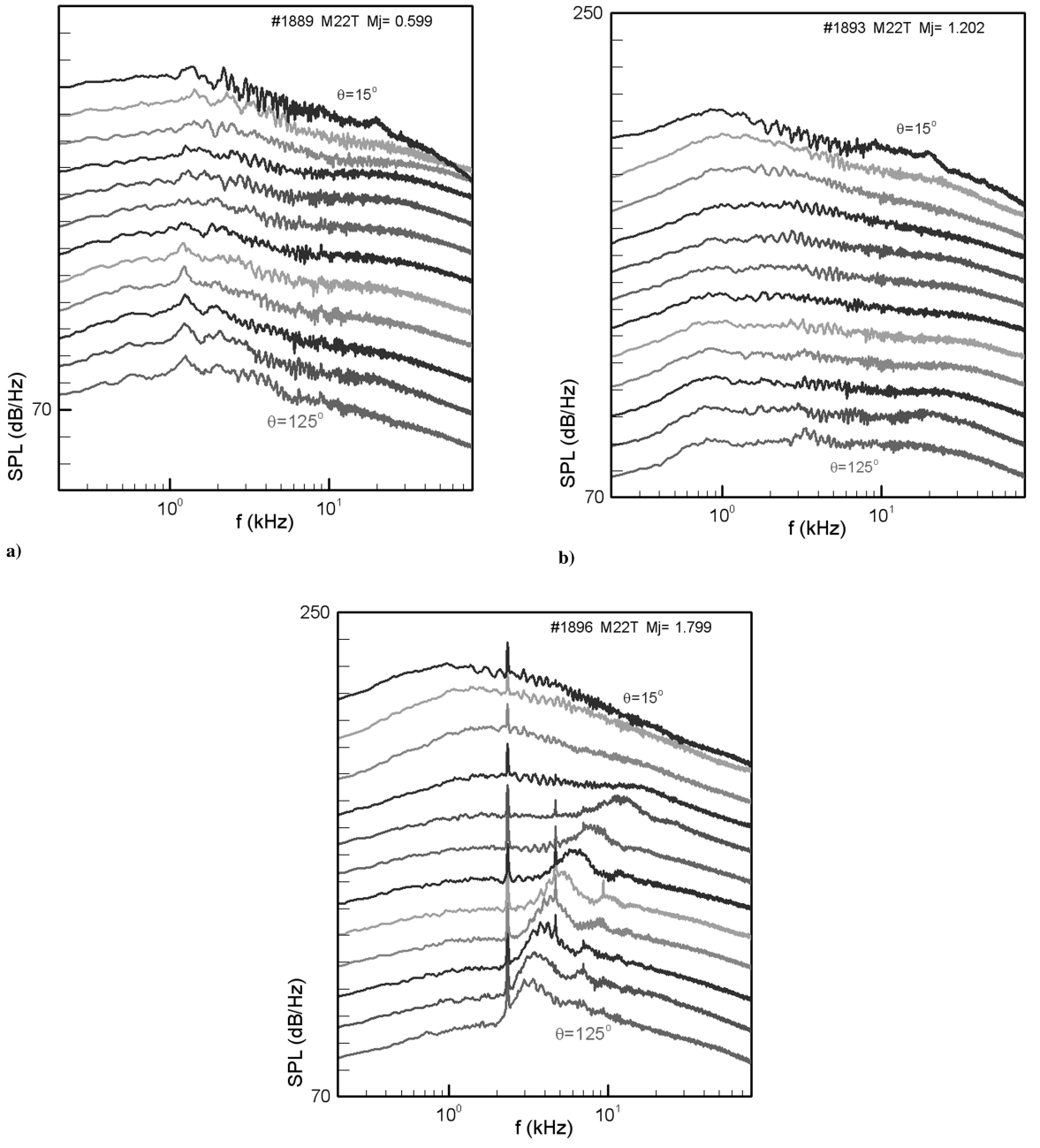

Fig. 9 SPL spectra for nozzle M22T (shown similarly in Fig. 5).

observed for the M28T case in Fig. 10 at $M_j = 0.6$. Thus, even with the boundary layer trip, residues of the transonic tone often persist. However, the spectra are by and large broadband in nature. It may also be noted that the trips do not affect screech or BBSN. This can be readily seen by comparing the spectra for $M_j = 1.8$ between Figs. 9 and 11.

The OASPL are calculated by integration of the spectra. OASPL for $\theta = 90$ deg are shown in Fig. 12 for the seven nozzle cases, as a function of M_j. For the convergent (M10T) case, the amplitudes are large for $M_j > 1.2$, partly due to screech. For M_j less than about 1, the levels are seen to be larger with the C–D nozzles. It is also clear that the increase in the level is more with the increasing design Mach number of the nozzle. These results confirm the overall trends reported in [1], based on data from the small nozzles. For the M22 case, there is an additional bulge due to the transonic tones. Ignoring the latter case, it is clear from the spectral traces that the excess noise occurs primarily due to an increase in the broadband levels.

In Fig. 12, the curves for M14, M16, and M18 cases are seen to involve a dip at $M_j = 1.4$, 1.6, and 1.8, respectively. These are the fully expanded conditions at which lower noise is expected, as discussed with Fig. 1. By inspecting the values given in Table 1, the following may also be noted. It can be inferred that for four of the C–D nozzles ($M_D > 1.4$), the shock is inside the divergent section at $M_j = 0.6$. Even though boundary II' (Fig. 4) was not measured for the present nozzles, the C–D cases are also likely to involve an internal shock at $M_j = 1.2$. At $M_j = 1.8$, on the other hand, the shock is thought to be outside for all cases. Thus, the EBBN is apparently characteristic of flows with a shock inside the divergent section.

Before proceeding with further results from the present experiment, a comparison is shown in Fig. 13, with data taken earlier with the same nozzles in another facility (CW17), that was given in the extended abstract of the conference version of this paper. The latter facility was semi-anechoic, and the data were taken with microphones only at $\theta = 90$ and 25 deg. OASPL versus M_j at $\theta = 90$ deg are compared for just three nozzles for clarity. It is noted that the amplitudes are somewhat different in the range $M_j > 1.2$, presumably because screech characteristics differed depending on

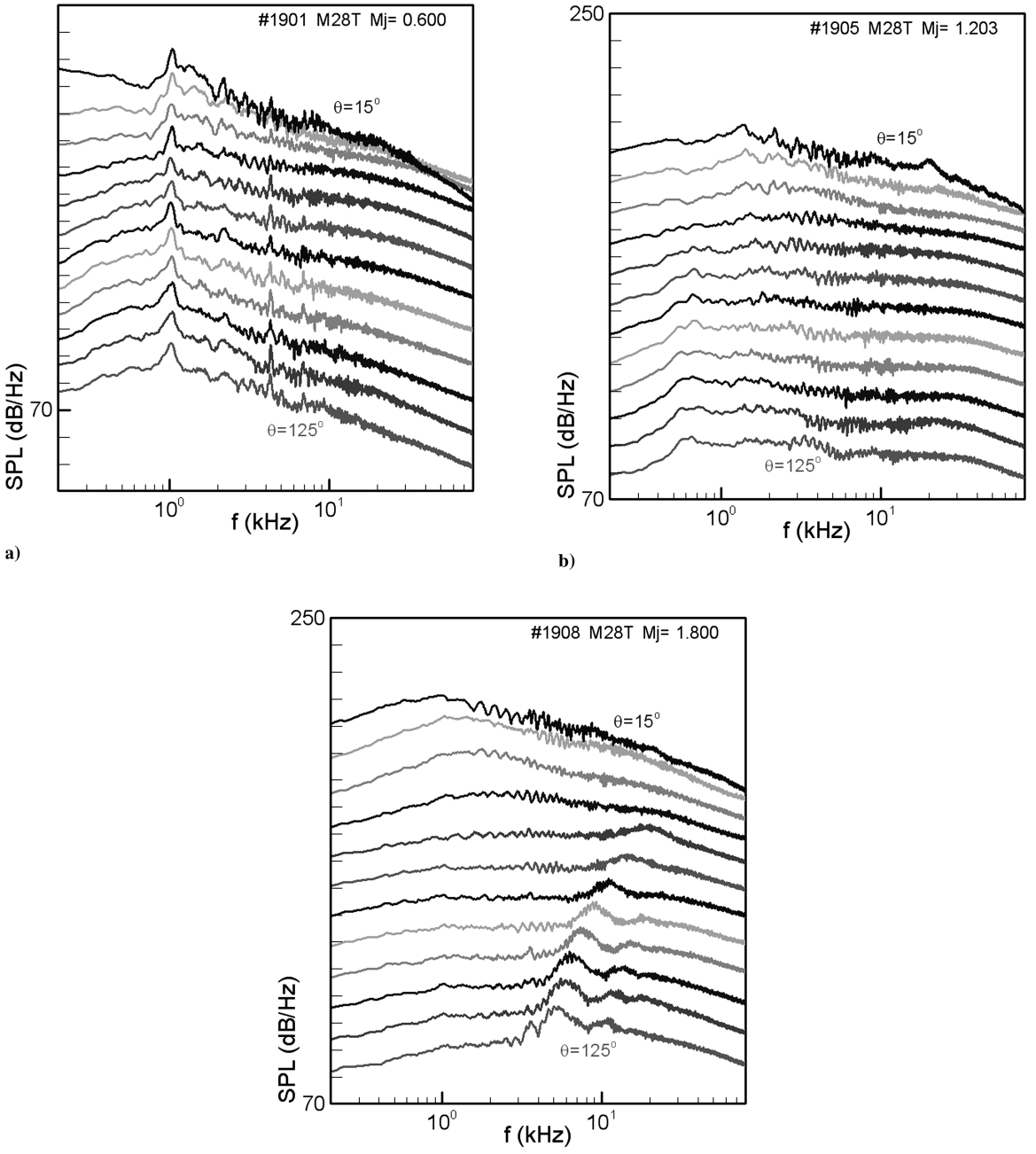

Fig. 10 SPL spectra for nozzle M28T (shown similarly in Fig. 5).

the details of the nozzle attachments and the facility geometry. At very low M_j, higher levels are indicated in CW17, apparently due to valve noise becoming relatively prominent. Nevertheless, the agreement is excellent over the range $0.5 < M_j < 1.2$, exhibiting the occurrence of the excess noise in either facility. This should put to rest any doubt that the EBBN could be spurious and facility dependent.

It is also noted here that the data presented in [1] for nozzles with simple conical divergent sections also exhibited a similar trend, as in Fig. 12. Nozzles having a larger divergence angle for the same length of the divergent section (hence, having a larger design Mach number based on the throat-to-exit area ratio) exhibited higher excess noise. However, when the design Mach number (or the divergence angle) is increased beyond a limit, the amplitudes drop back, as discussed further in the following.

OASPL data corresponding to Fig. 12 are shown in Fig. 14 for a shallow angle, $\theta = 25$ deg. The occurrence of EBBN can be observed; however, the threshold of M_j below which it occurs is found to be lower. Also, the increases in the levels are smaller. These data trends become clearer with the directivity plots shown in the following. In Fig. 14, it is also noted that the levels for the M28T case are significantly lower at high M_j. Corresponding levels for M22 and M22T cases are also low. This is apparently due to lower flow rates with the higher M_D nozzles because the throat diameters are smaller. Note that with the M28 nozzle, the throat diameter is about half, and thus the mass flow rate is about one-fourth relative to the convergent case for a given NPR (or M_j). Massive boundary layer separation within the divergent section is also expected with the higher M_D nozzles.

Directivity plots (OASPL vs θ) are shown in Figs. 15–18, for four values of M_j (0.6, 1.0, 1.4, and 1.8). In each figure, the OASPL data (as measured) are shown for the six nozzles. At $M_j = 0.6$, in Fig. 15, the occurrence of EBBN is abundantly clear, with the three nozzles having the largest design Mach number. Insignificant differences are noted among data from the M10T, the M14T, and the M16T cases. The amplitudes increase clearly with M18T and there is a large further increase with M22T, but the amplitudes fall back somewhat with the M28T nozzle. As discussed in the previous

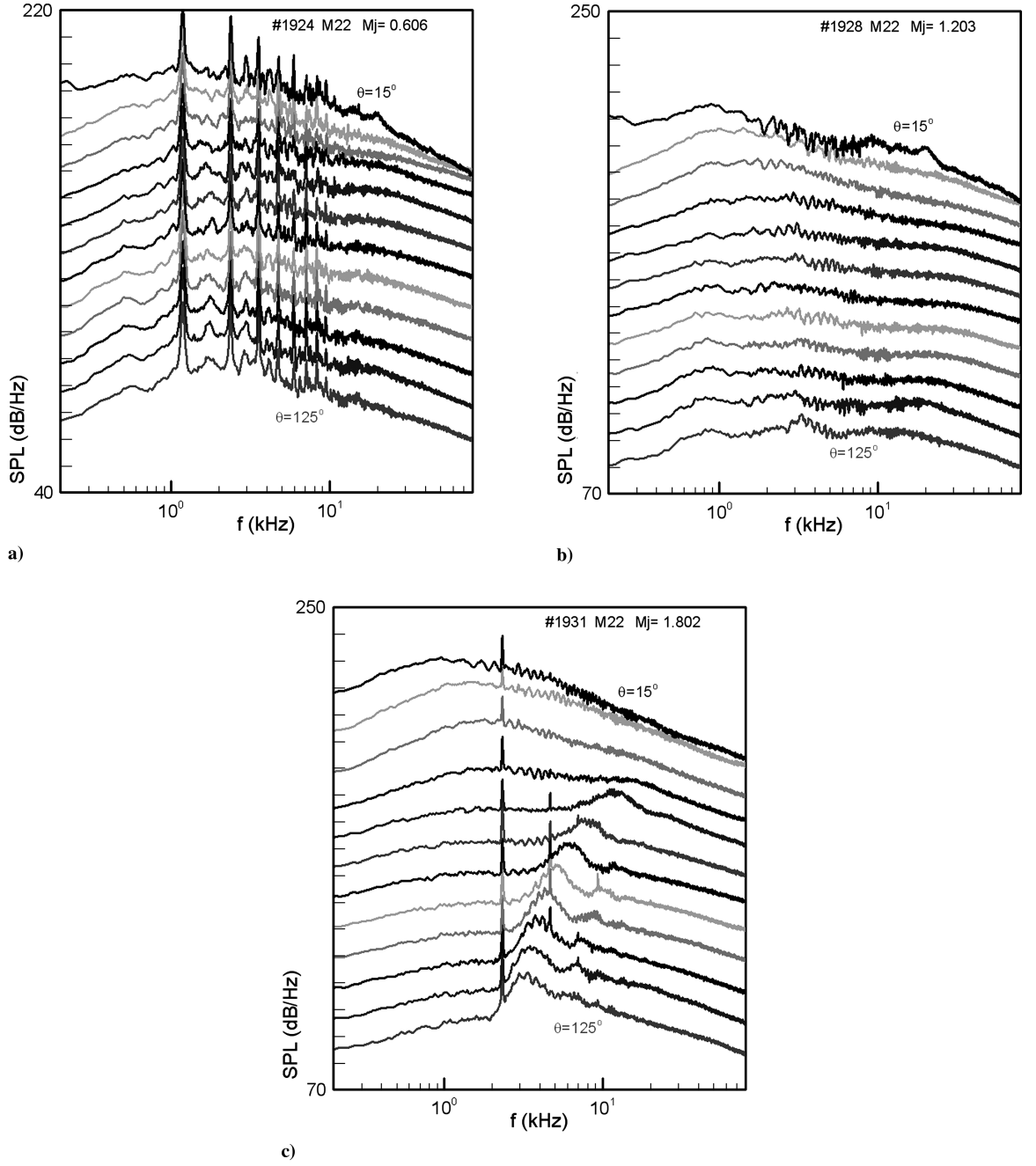

Fig. 11 SPL spectra for nozzle M22 (shown similarly in Fig. 5).

paragraph, the mass flow rate with the M28T nozzle is about one-fourth of that with the convergent nozzle. A huge increase in the noise takes place in spite of the smaller flow rate. However, in the limit $M_D \to \infty$, the mass flow rate, and hence the noise, would tend to be zero, and a reversal in the trend of increasing noise with increasing M_D is naturally expected. This reversal has apparently ensued when going from the M22 to the M28 case. In Fig. 15, it can also be seen that at shallow angles, the relative increase in OASPL is small. This provides a clearer perspective with regards to the lower amplitudes noted in Fig. 14. At $M_j = 1.0$, in Fig. 16, EBBN is also quite prominent, and similar trends are noted, as seen in Fig. 15. Here, the M14T and M16T nozzles are also seen to involve higher amplitudes at larger values of θ. However, overall, the increases in the levels relative to the convergent case are not as large as seen at $M_j = 0.6$.

Directivity data for $M_j = 1.4$ and 1.8 are shown in Figs. 17 and 18, respectively. The data trends become obscure, partly because of the occurrence of screech and BBSN. The M10T and M16T cases have the largest amplitudes, and there is no evidence of excess OASPL with the C–D nozzles. In Fig. 17, the flow is fully expanded at $M_j = 1.4$ with the M14T nozzle. Thus, corresponding amplitudes are found to be generally low, as expected. This is especially true at the high end of the θ range, at which the noise from the imperfectly expanded jets is dominated by screech and BBSN. The amplitudes are seen to be smaller at shallow angles, with the two nozzles having the largest M_D due to reasons already explained. Essentially, the same comments can be made from Fig. 18, in which the M18T nozzle has fully expanded flow and hence the least noise.

The data presented so far are as measured. Would the trends for EBBN be different had the throat diameters been used for data normalization? That is, would the relative levels be different if the throat diameter, instead of the exit diameter, were kept constant in the experiment? This is examined in Fig. 19, in which the data of Fig. 16 are replotted with the intensity normalized as $I^* = I(D_e/D_t)^2$. As expected, the excess amplitudes have become amplified and more prominent. The same conclusion is reached when the data of Fig. 12 are scaled by the throat diameters, as shown in Fig. 20. The increases in the noise levels with the present nozzles, shown with the OASPL values as measured, are thus

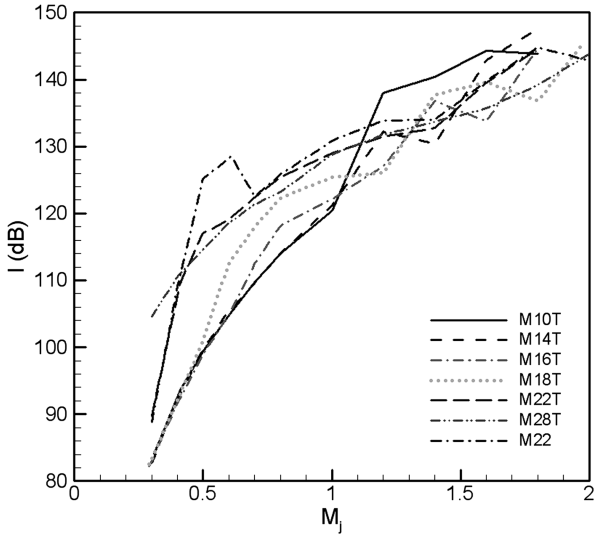

Fig. 12 OASPL at $\theta = 90$ deg, as a function of M_j for all nozzles.

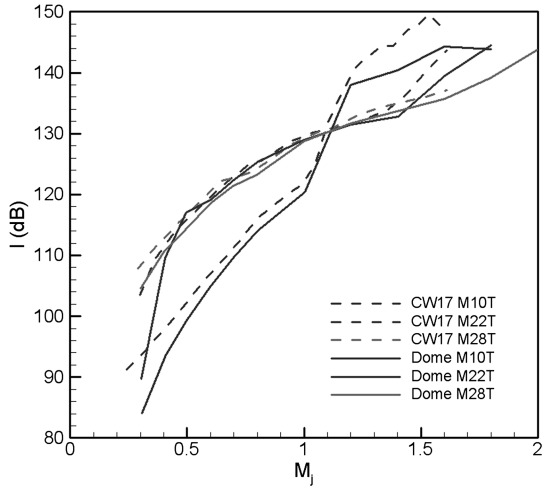

Fig. 13 OASPL at $\theta = 90$ deg, as a function of M_j for three nozzles, as indicated. Comparison of present data (dome) with data taken earlier in another facility (CW17).

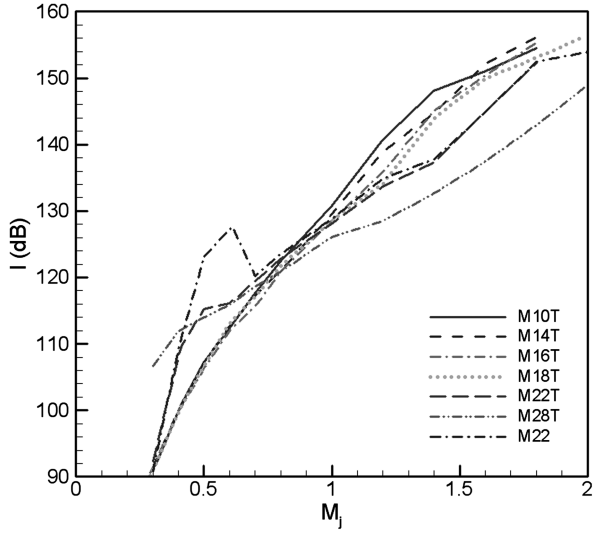

Fig. 14 OASPL at $\theta = 25$ deg, as a function of M_j for all nozzles.

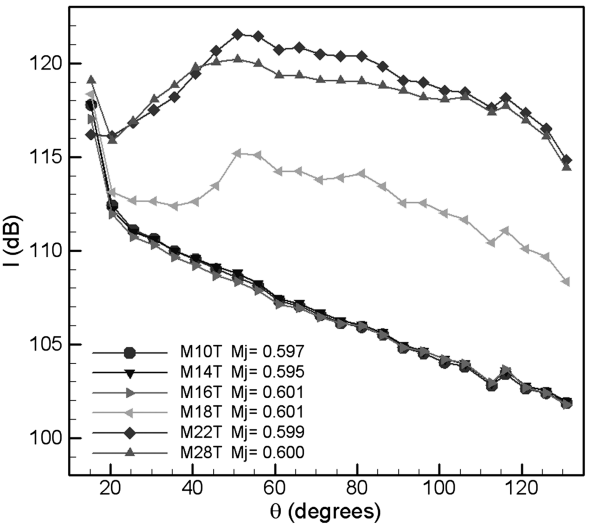

Fig. 15 OASPL vs θ for different nozzles, as indicated; $M_j \approx 0.6$.

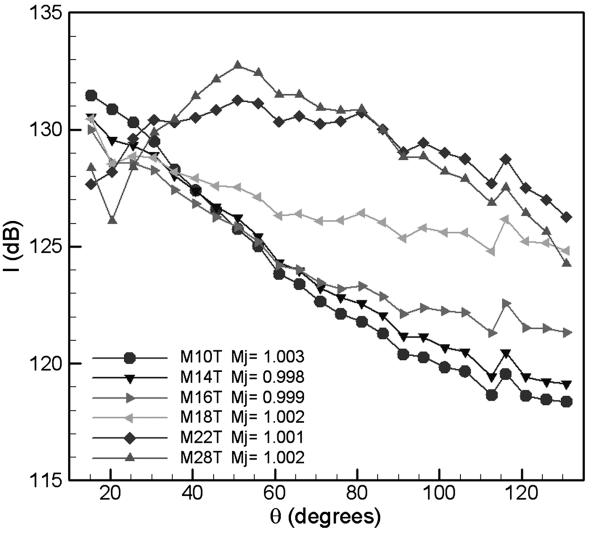

Fig. 16 OASPL vs θ for different nozzles, as indicated; $M_j \approx 1.0$.

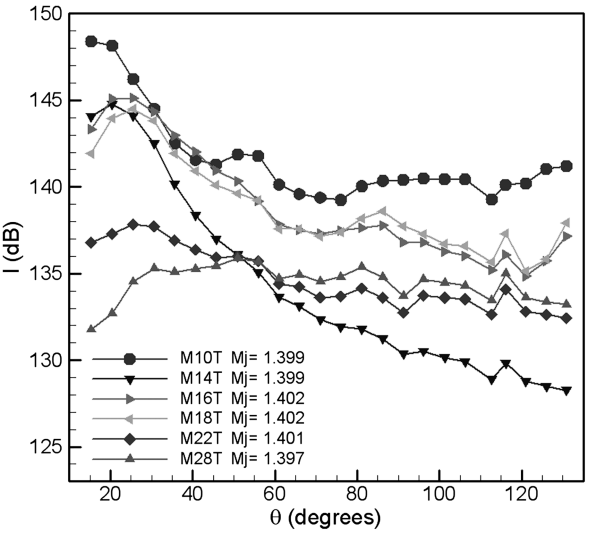

Fig. 17 OASPL vs θ for different nozzles, as indicated; $M_j \approx 1.4$.

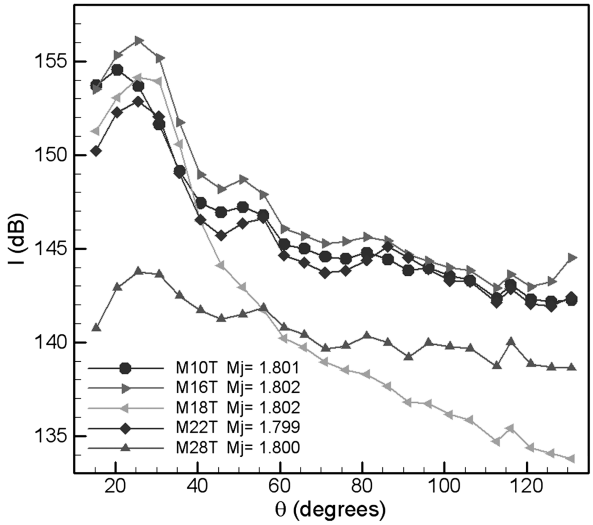

Fig. 18 OASPL vs θ for different nozzles, as indicated; $M_j \approx 1.8$.

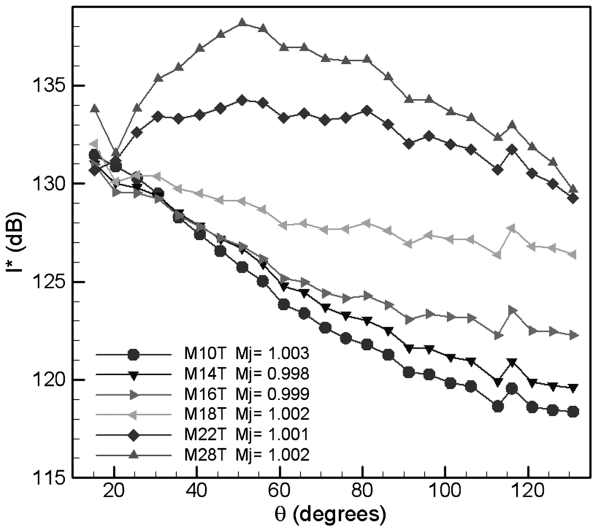

Fig. 19 OASPL, normalized by throat diameter, vs θ for different nozzles; $M_j \approx 1.0$ (data corresponding to Fig. 16).

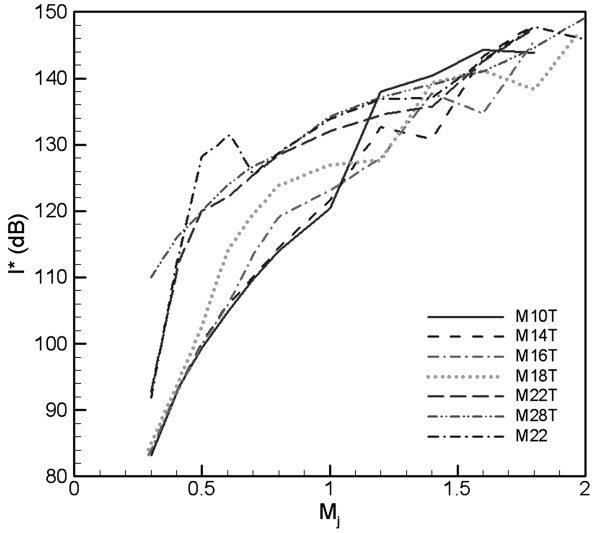

Fig. 20 OASPL, normalized by throat diameter, vs M_j for different nozzles; $\theta = 90$ deg (data corresponding to Fig. 12).

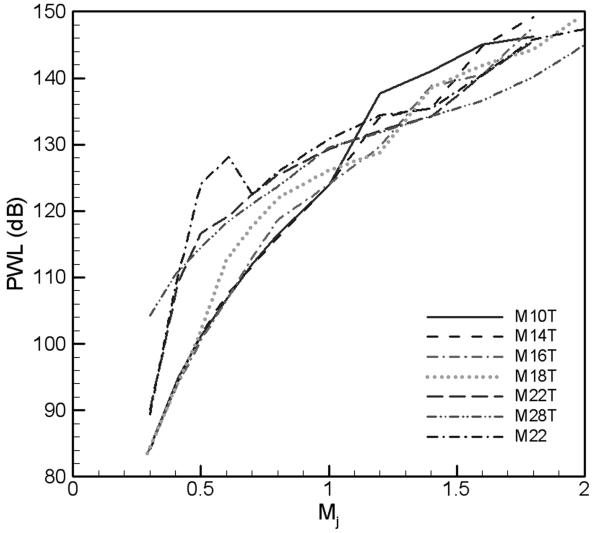

Fig. 21 Relative PWL of radiated noise vs M_j for different nozzles.

conservative. That the C–D nozzles are noisier in the low M_j range due to EBBN is established beyond any doubt.

Finally, the overall power levels (PWL) are calculated by integration of the data from the 24 microphones. The PWL data are shown in Fig. 21. The trends are essentially the same as seen with the OASPL data for $\theta = 90$ deg (Fig. 12). Thus, the total power of the radiated sound is high in the M_j range in which EBBN occurs, and the phenomenon is not just characteristic of specific angular locations.

IV. Conclusions

Results of an experiment on the characteristics of an excess noise occurring with C–D nozzles in the overexpanded regime are presented in this paper. Data are obtained with five C–D nozzles and compared with that from a convergent nozzle. The results clearly establish that the C–D nozzles are noisier in the low Mach number range of the overexpanded regime. This is shown by comparison of the spectral data, directivity patterns as well as overall radiated power calculations. The excess amplitude is most pronounced around $\theta = 45$ deg and is prominent at larger angles. At shallow angles near the jet's downstream edge, it may not be clearly noticed.

The excess noise occurs even if there are no tones present, and the spectral distribution is broadband, hence the term EBBN. With earlier results shown in [1], it is clear that the EBBN takes place roughly in the same M_j range in which transonic tones are expected, with a nozzle having a smooth interior. This leads to the belief that EBBN and the transonic tones are similar in morphology. Both trace to unsteady shock motion within the divergent section. With a smooth interior, providing azimuthal symmetry, the unsteady shock motion locks on to a resonance generating the transonic tones. With a larger practical nozzle, or boundary layer trip with the model-scale nozzles, a breakdown in azimuthal symmetry apparently prevents the resonance leading to a random unsteady motion. The latter gives rise to the observed increase in the noise levels that are broadband in nature.

The periodic shock motion associated with the transonic tone was documented in some detail in [5]. The shock would not only change axial position but also change significantly in shape and strength within the period of the tone. The details of the shock unsteadiness associated with EBBN remain uncharted. It is possible that the unsteadiness is similar to that seen with the transonic tone, albeit with superimposed randomness. Although the transonic tone is similar to one-quarter-wave acoustic resonance [5], the EBBN may also be contributed by shock boundary layer interaction and possible unsteadiness of a separation bubble that might be present downstream of the shock. If the latter were the dominant mechanisms, perhaps flow control within the divergent section would have a chance to

suppress EBBN. However, these possibilities remain conjectures at this time, and further experimentation would be needed for a full understanding and possible control.

With reference to the objectives enumerated in Sec. I, it may be noted that the EBBN is now demonstrated with larger well-designed C–D nozzles. Because the exit diameter of the present nozzles is a constant, higher M_D involves smaller throat diameter and hence smaller flow rate at a given pressure ratio (i.e., given M_j). Thus, large excess noise can occur even though the flow rate is smaller. For example, with the $M_D = 2.8$ nozzle (relative to the convergent case) a 13 dB increase in OASPL occurs at $M_j = 0.6$ even though the mass flow rate is about one-fourth. The excess noise at a given M_j is found to be more prominent with nozzles of a larger design Mach number (M_D). Obviously, there should be a limiting M_D when the trend of increasing noise with increasing M_D should reverse because, in the limit of $M_D = \infty$, the flow rate and noise would tend to be zero. This reversal is noticed at the highest M_D (2.8) covered in the present experiment.

As discussed in [1], the EBBN is distinct in characteristics from BBSN. A clear trend of BBSN, as also documented in the Appendix of the present paper, is a decreasing frequency of the peak with increasing angular location. This is not the case with EBBN, and the spectral shape appears more or less similar in all directions. It is possible that EBBN and BBSN are mutually exclusive. With a given C–D nozzle, when one occurs, the other may not. BBSN occurs when the shock from the divergent section is pushed out and a periodic train of strong shocks is formed outside the nozzle. On the other hand, EBBN occurs at lower pressure ratios when the shock is inside.

How relevant is EBBN in practical applications? Because it occurs at lower pressure ratios at the onset of the overexpanded regime, it may not be of concern in typical flight conditions. This might be the reason why the phenomenon, to the best of our knowledge, has gone practically unrecognized in the vast literature on jet noise. However, there could be situations [e.g., the climb-to-cruise stage of certain fighter jets when the engine involves overexpanded exhaust [7–9] and rocket nozzles in a launch pad environment (see, for example, [10])] in which it might be relevant. It is needless to say, however, that one must be aware of its existence, especially in efforts to simulate and predict supersonic jet noise accurately.

Appendix: Mass Flow Rate and Broadband Shock Associated Noise Peak Frequency

Figures A1 and A2 are included as side observations made during the course of this investigation. Figure A1 shows measured mass flow rate in comparison to 1-D nozzle flow calculations. The agreements are found to be excellent. It was thought that with massive flow separation for the large M_D cases, there might be some difference. Apparently, the throat and the pressure ratio determine the mass flow rates that are not impacted by flow separation within the divergent section. Only, at very low M_j, a significant difference is noted, especially for the M28T case. Presumably, the separation location encroaches far enough upstream to affect the throat characteristics.

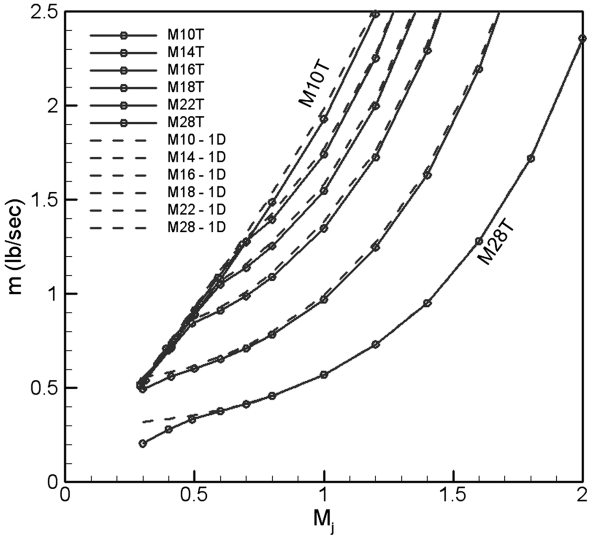

Fig. A1 Mass flux vs M_j: measured data (solid lines) compared with 1-D nozzle flow prediction (dashed lines).

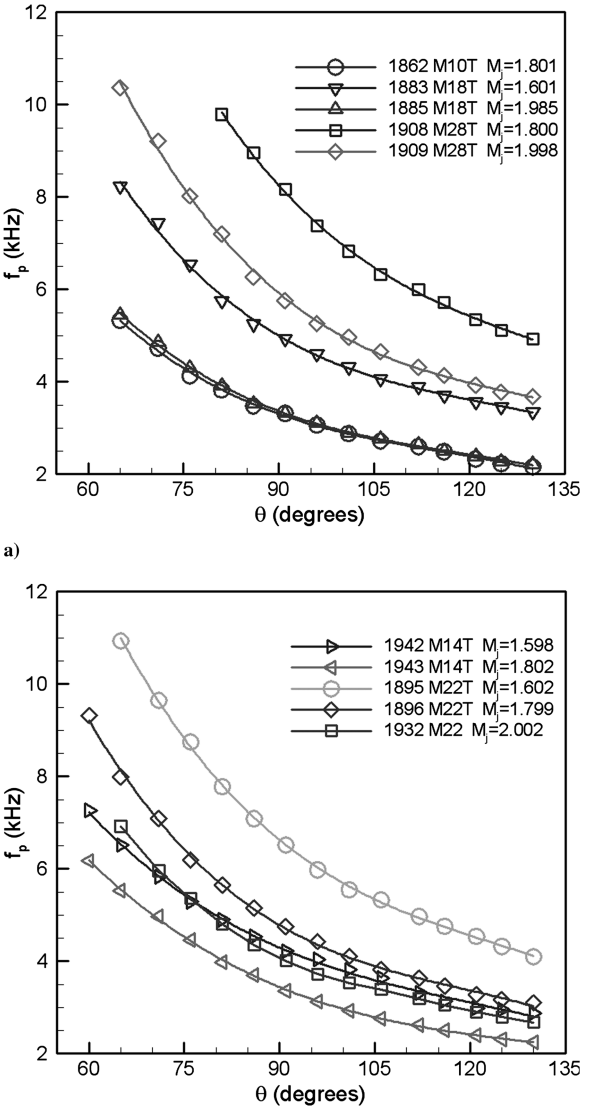

Fig. A2 BBSN peak frequency vs θ. Data are shown in two sets for clarity: a) M10T, M18T, and M28T cases and b) M14T and M22T cases.

As mentioned during the discussion of Fig. 6, the BBSN peak frequencies f_p were approximately read off from the data wherever they were clear. The variations of f_p with θ are shown in Fig. A2. For clarity, the data are shown in two sets, as identified in the legends. A decreasing f_p with increasing θ is a characteristic of BBSN, observed and explained in [2,11]. No attempt is made in this paper to compare these data with available predictions.

Acknowledgment

Support from the Supersonic Project under the Fundamental Aeronautics Program is gratefully acknowledged.

References

[1] Zaman, K. B. M. Q., "Noise Characteristics of Overexpanded Jets from Convergent–Divergent Nozzles," 46th Aerospace Sciences Meeting, AIAA Paper 2008-25, Jan. 2008.

[2] Tam, C. K. W., and Tanna, H. K., "Shock Associated Noise Of Supersonic Jets From Convergent–Divergent Nozzles," *Journal of Sound and Vibration*, Vol. 81, No. 3, 1982, pp. 337–358. doi:10.1016/0022-460X(82)90244-9

[3] Tam, C. K. W., "Supersonic Jet Noise," *Annual Review of Fluid Mechanics*, Vol. 27, Jan.–1995, pp. 17–43. doi:10.1146/annurev.fl.27.010195.000313

[4] Bridges, J. E., and Brown, C. A., "Validation of the Small Hot Jet Acoustic Rig for Jet Noise Research," AIAA Paper 2005-2846, 2005.

[5] Zaman, K. B. M. Q., Dahl, M. D., Bencic, T. J., and Loh, C. Y., "Investigation of a 'Transonic Resonance' with Convergent–Divergent Nozzles," *Journal of Fluid Mechanics*, Vol. 463, No. 1, 2002, pp. 313–343. doi:10.1017/S0022112002008819

[6] Hunter, C. A., "Experimental, Theoretical, and Computational Investigation of Separated Nozzle Flows," AIAA Paper 98-3107, 1998.

[7] Greska, B., Krothapalli, A., and Arakeri, V., "A Further Investigation into the Effects of Microjets on High Speed Jet Noise," 9th AIAA/CEAS Aeroacoustics Conference, AIAA Paper 2003-3128, May 2003.

[8] Norum, T. D., Garber, D. P., Golub, R. A., Santa Maria, O. L., and Orme, J. S., "Supersonic Jet Exhaust Noise at High Subsonic Flight Speed," NASA TP 2004-212686, Jan. 2004.

[9] Seiner, J. M., Jansen, B. J., and Ukeiley, L. S., "Acoustic Fly-Over Studies of F/A E/F Aircraft During FCLP Mission," 9th AIAA/CEAS Aeroacoustics Conference, AIAA Paper 2003-3330, May 2003.

[10] Kandula, M., "Prediction of Turbulent Jet Mixing Noise Reduction by Water Injection," *AIAA Journal*, Vol. 46, No. 11, 2008, pp. 2714–2722. doi:10.2514/1.33599

[11] Harper-Bourne, M., and Fisher, M. J., "The Noise from Shock Waves in Supersonic Jets," *Proceedings of the AGARD Conference on Noise Mechanisms*, AGARD CP 131, 1973.

E. Gutmark
Associate Editor